Available online at www.sciencedirect.com
ScienceDirect
Catalysis Today 130 (2008) 471–485
CATALYSIS TODAY
www.elsevier.com/locate/cattod

Hydrogenation of naphthalene on NiMo- Ni- and Ru/Al_2O_3 catalysts: Langmuir–Hinshelwood kinetic modelling

Ana Cristina Alves Monteiro-Gezork [a,*], Reyna Natividad [b], John Mike Winterbottom [a]

[a] *Department of Chemical Engineering, School of Engineering, The University of Birmingham, Birmingham B15 2TT, United Kingdom*
[b] *Department of Chemical Engineering, Faculty of Chemistry, Universidad Autónoma del Estado de México, Paseo Colón Esq. Tollocan, Toluca, Edo. de México, México CP 50120, Mexico*

Abstract

The importance of the hydrodearomatisation (HDA) is increasing together with tightening legislation of fuel quality and exhaust emissions. The present study focuses on hydrogenation (HYD) kinetics of the model aromatic compound naphthalene, found in typical diesel fraction, in *n*-hexadecane over a NiMo (nickel molybdenum), Ni (nickel) and Ru (ruthenium) supported on trilobe alumina (Al_2O_3) catalysts. Kinetic reaction expressions based on the mechanistic Langmuir–Hinshelwood (L–H) model were derived and tested by regressing the experimental data that translated the effect of both naphthalene and hydrogen concentration at a constant temperature (523.15 and 573.15 K over the NiMo catalyst and at 373.15 K over the Ni and Ru/Al_2O_3 catalysts) on the initial reaction rate. The L–H equation, giving an adequate fit to the experimental data with physically meaningful parameters, suggested a competitive adsorption between hydrogen and naphthalene over the presulphided NiMo catalyst and a non-competitive adsorption between these two reactants over the prereduced Ni and Ru/Al_2O_3 catalysts. In addition, the adsorption constant values indicated that the prereduced Ru catalyst was a much more active catalyst towards naphthalene HYD than the prereduced Ni/Al_2O_3 or the presulphided $NiMo/Al_2O_3$ catalyst.

Keywords: Naphthalene hydrogenation; Kinetic modelling; $NiMo/Al_2O_3$; Ni/Al_2O_3; Ru/Al_2O_3

1. Introduction

Hydrotreatment is an important group of processes in the petroleum refining industry for (1) the protection of the catalysts used in latter stages of the refining process, (2) the abatement of NO_x and SO_2 emissions that could arise from the combustion of organic molecules, (3) the improvement of the properties of the final products issued from refining (such as colour, smell and stability) and (4) the valorisation of heavy stocks. It is an extensively documented process and several reviews have been devoted to it during the last decades [1–5]. Due to the required use of new feedstocks and application of more severe environmental legislation [6], the interest on this subject is constantly renewed. During the hydrotreating process, the HYD of the aromatic rings prior to sulphur removal is considered to alleviate the steric hindrance of substituted dibenzothiophenes, considered the most unreactive towards hydrodesulphurisation (HDS), and therefore facilitate HDS reaction [5,7]. Moreover, nitrogen removal from polycyclic aromatics does not take place until ring saturation has occurred. A high aromatic content is associated with poor fuel quality, giving a low cetane number in diesel fuel and a high smoke point in jet fuel [8,9]. Consequently, from the viewpoint of environmental conservation, aromatics saturation is the key reaction to reduce NO_x and particulate matter [10] in order to provide environmentally more acceptable reformulated fuels.

Aromatic HYD in industrial feedstocks may be carried out over supported metal or metal sulphided catalysts. NiMo catalyst is a typical hydrotreating catalyst that is commonly used in industry to catalyse primarily HDA and secondly HDS reactions, whether in a single stage process or in the first stage of a two-stage process. In a two-stage process, the HDA is usually achieved in the second stage with Ni or noble metal catalysts [11]. Presulphided NiMo catalysts are reported to be resistant to sulphur and coke deposition, whereas supported Ni or noble metal catalysts should be used in a sulphur-free

* Corresponding author. Present address: Stühlinger Straße 17, 79106 Freiburg, Germany.
E-mail address: acm848@yahoo.com (A.C.A. Monteiro-Gezork).

0920-5861/$ – see front matter © 2007 Elsevier B.V. All rights reserved.
doi:10.1016/j.cattod.2007.10.102

Nomenclature

b_i	adsorption equilibrium constant of component i ($m_L^3\ mol^{-1}$)
C	concentration ($mol\ m_L^{-3}$)
DMDS	dimethyldisulphide
HDA	hydrodearomatisation
HDS	hydrodesulphurisation
HYD	hydrogenation
k_3, k_{-3}	rate constants of the forward and reverse reaction of step III (units depend on the rate expression)
k_4, k_{-4}	rate constants of the forward and reverse reaction of step IV (units depend on the rate expression)
K	rate equilibrium constant
N	naphthalene
Rc	regression coefficient
$r_{w,i}$	reaction rate per mass of catalyst or active phase relative to component i, $mol\ kg_{cat}^{-1}\ s^{-1}$ ($mol\ kg_{NiMo}^{-1}\ s^{-1}$)
$(SSR)_{min}$	minimised sum of squares of residuals
S_{td}	standard deviation
T	temperature (K)

Greek letters

η	effectiveness factor
σ_{ij}	correlation coefficient between parameter i and parameter j

Subscripts and superscripts

calc	calculated
cat	catalyst
exp	experimental
H, H_2	atomic and molecular hydrogen
L	liquid (bulk)
N	naphthalene
obs	observed
T	tetralin

environment, in order to fully make use of its HDA properties [12].

Covering all types of catalysts used for HDA, a conventional NiMo catalyst, a Group VIII Ni and an in-house noble catalyst, Ru, all supported on trilobe Al_2O_3 have been investigated for the HYD of naphthalene in *n*-hexadecane. In view of the interest in describing and comparing the reaction mechanism over these three catalysts, L–H rate expressions were developed and tested. The experimental data that translated the effect of both naphthalene and hydrogen concentration at a constant temperature on the initial reaction rate was regressed using a non-linear least squares method and the adsorption parameters were estimated.

2. Experimental methods

2.1. Apparatus

The kinetic study was carried out in two identical reactors. One of the reactors was contaminated by sulphur and was used only for the reactions performed over the presulphided NiMo/Al_2O_3 catalyst. The other reactor was sulphur free and was used for the reactions performed over the prereduced Ni and Ru/Al_2O_3 catalysts. Both reactors were three-phase spinning catalyst basket autoclave reactors and were operated as a dead-end mode. In order to maintain the reactor pressure constant, the hydrogen was supplied continuously to the reactor at the rate it was consumed by the reaction. The reactors were automated and controlled to ensure reliable and reproducible experiments. A more detailed description of the two apparatus is given elsewhere [13].

2.2. Catalysts and materials

The catalysts used in this research were commercial Al_2O_3 trilobe support-based catalysts namely NiMo/Al_2O_3 (25.9 wt% MoO_3, 5.45 wt% NiO, 4.06 wt% P_2O_5, Grace Davison), Ni/Al_2O_3 (15.5 wt% Ni, HTC 400 RP Johnson Matthey) and an in-house made Ru/Al_2O_3 catalyst (1.9 wt% Ru, Johnson Matthey). The NiMo/Al_2O_3 catalyst was used in a presulphided form and the Ni and Ru/Al_2O_3 catalysts in a prereduced one. The pretreatment of the catalysts is described elsewhere [12,13]. For all the experiments presented in this study, a mass of 35.2×10^{-3}, 21.5×10^{-3} and 7.5×10^{-3} kg_{cat} was used for the NiMo, Ni and Ru/Al_2O_3 catalysts, respectively.

As a feed, naphthalene (99%, Aldrich) was dissolved in *n*-hexadecane (99%, Avocado) to the required concentration and *n*-octadecane (99%, Aldrich) was used as an internal standard. With the presulphided NiMo/Al_2O_3 catalyst, dimethyldisulphide, DMDS (99%, Acros) was added to the reaction mixture, providing a source of sulphur that was essential to stabilize the catalyst maintaining it in the sulphided form [12,13]. Liquid products were analysed using a gas chromatograph (Ai Cambridge GC, model GC94M) equipped with a capillary column (CP-Wax 52CB FS 25 × 0.25(1.2), Chrompack). The nitrogen (oxygen-free), argon (Ar), air, hydrogen (H_2) and helium (>99.995%) cylinder gases were supplied by BOC Gases. The helium was purified by passing it through an oxygen/moisture trap and the hydrogen was filtered prior to the HYD reactions.

2.3. Experimental program

The effect of hydrogen partial pressure and naphthalene concentration in the feed at a constant temperature on the initial HYD rate of naphthalene, over the presulphided NiMo catalyst and over the prereduced Ni and Ru/Al_2O_3 catalysts, was studied. From the catalytic activity measurements, an initial reaction rate was determined by calculating the hydrogen consumption during the initial stage of the reaction, i.e., when no significant amount of tetralin formation was observed (naphthalene conversion < 10%). The same batch of presulphided NiMo/Al_2O_3 catalyst was used throughout this work. A standard experiment, carried out at 15×10^5 Pa hydrogen partial pressure and 573.15 K, was performed repeatedly between experiments to ensure experimental reproducibility and to ensure that no catalyst deactivation occurred. On the

other hand, a fresh batch of Ni and Ru/Al_2O_3 catalysts was used for each experiment.

3. Results and discussion

The kinetic data were acquired by Monteiro-Gezork et al. [13] by investigating the effect of several operating parameters on the initial HYD rate of naphthalene, over the presulphided NiMo catalyst and over the prereduced Ni and Ru/Al_2O_3 catalysts. The initial reaction rate was found to increase with increased initial concentration of naphthalene ($\approx 90 - 600\,\mathrm{mol_N\,m_L^{-3}}$), over the three catalysts and with increased hydrogen partial pressure ($P_{H_2} = (5-30) \times 10^5$ Pa) over the NiMo and Ni/Al_2O_3 catalysts at a constant temperature (523.15 and 573.15 K over the NiMo catalyst and 373.15 K over the Ni and Ru/Al_2O_3 catalysts). However, in the case of Ru/Al_2O_3, the reaction rate increased up to a hydrogen partial pressure of 20×10^5 Pa and no change was observed as it increased further to 30×10^5 Pa. Intrinsic kinetics were observed over the $NiMo/Al_2O_3$ catalyst at 523.15 K. However, the intraparticle resistances could not be avoided over this catalyst at 573.15 K and over the Ni and Ru/Al_2O_3 catalysts at 373.15 K. An effectiveness factor, η, was estimated for the three catalysts using the Weisz and Prater criterion [14]. A more detailed description of the method used can be found elsewhere [13]. The η values found were 0.67 for the $NiMo/Al_2O_3$ catalyst at 573.15 K and 0.14 and 0.15 for Ni and Ru/Al_2O_3 catalysts at 373.15, respectively. In the present work, the above-described experimental data will be used for the L–H modelling. The η values found by Monteiro-Gezork et al. [13] will be taken into consideration in the L–H rate expressions.

3.1. L–H mechanism for naphthalene hydrogenation

The kinetic model was based on the following surface reaction mechanism proposed earlier by Smeds et al. [15] for the gas-phase HYD of ethylbenzene and extensively used for liquid-phase HYD of other aromatic hydrocarbons such as naphthalene [16,17]. The mechanism consists of aromatics and hydrogen adsorption steps, consecutive hydrogen addition steps and product desorption steps. According to isotopic transient studies [18], hydrogen is added pairwise, either in the form of atoms or molecules and this was also taken into account.

$$\mathrm{N} + * \overset{b_N}{\longleftrightarrow} \mathrm{N}^* \quad \text{(I)}$$

$$2\mathrm{H}_2 + 2\gamma^\bullet \overset{b_H}{\longleftrightarrow} 2\gamma\mathrm{H}^\bullet_{2/\gamma} \quad \text{(II)}$$

$$\mathrm{N}^* + \gamma\mathrm{H}\cdot_{2/\gamma} \overset{K_3}{\longleftrightarrow} \mathrm{NH}_2^* + \gamma\cdot \quad \text{(III)}$$

$$\mathrm{NH}_2^* + \gamma\mathrm{H}^\bullet_{2/\gamma} \overset{K_4}{\longleftrightarrow} T^* + \gamma^\bullet \quad \text{(IV)}$$

$$T^* \overset{1/b_T}{\longleftrightarrow} T + * \quad \text{(V)}$$

where N is naphthalene, T is tetralin, H_2 is molecular hydrogen, H is atomic hydrogen and $NH_2{}^*$ is the adsorbed intermediate; $\gamma = 1$ for molecular adsorption of hydrogen and $\gamma = 2$ for dissociative adsorption; $^\bullet$ and * denote the active sites for hydrogen and naphthalene, respectively; b_N, $b_{H_{2/\gamma}}$ and b_T are the adsorption equilibrium constants for naphthalene, hydrogen (atomic or molecular) and tetralin, respectively; $K_3 = k_3/k_{-3}$ and $K_4 = k_4/k_{-4}$ are the rate equilibrium constants of step III and IV, respectively; k_3, k_{-3} and k_4, k_{-4} are the rate constants of the forward and reverse reaction of steps III and IV, respectively. For the case of competitive adsorption, the sites $^\bullet$ and * coincide.

In deriving the plausible rate expressions of the L–H-type model from mechanism (I)–(V) for the reaction of naphthalene with hydrogen, some fundamental assumptions were introduced and 14 possible mechanisms, or combinations of mechanisms, were considered and evaluated. These included as reaction-determining steps, either surface reaction or adsorption of hydrogen or naphthalene with combinations of (a) adsorption of naphthalene and hydrogen on the same type of catalyst site (competitive adsorption); (b) involvement of two types of catalyst sites, one for adsorption of hydrogen, the other for naphthalene (non-competitive adsorption); and (c) dissociative (atomic) adsorption of hydrogen in contrast to molecular adsorption. It was assumed that the rate-determining step was irreversible. The derived rate expressions are summarized in Table A.1 in Appendix A. For low conversions of naphthalene, tetralin concentration is small and therefore, the rate of HYD of naphthalene is reduced to the initial one. The corresponding expressions for this simplification are also presented in Table A.1. The solvent did not adsorb on the catalyst and consequently an adsorption term for the solvent is not included in any of the derived kinetics expressions.

3.2. Parameter estimation

In all, 14 different models were examined for their ability to describe the experimental data. In order to select a suitable rate equation among those aforementioned, a non-linear least squares regression analysis was used for each rate equation in order to obtain the best values of the adsorption and kinetic parameters. The parameter estimation was performed by minimizing the sum of squares of residuals (SSR) of the differences between the experimental and the calculated initial reaction rates, $r_{w,N,exp}$ and $r_{w,N,calc}$, respectively:

$$\mathrm{SSR} = \sum_i \left(r_{w,N,exp} - r_{w,N,calc}\right)^2$$

Minimization was carried out with the optimisation program Mathematica™ 5 that uses the Marquardt method [19]. The L–H models were tested by regressing the experimental data that translated the effect of both naphthalene and hydrogen concentration at a constant temperature on the initial reaction rate. In the minimization process, the concentration of naphthalene and the concentration of hydrogen were the independent variables and the experimental reaction rate was the dependent variable. The experimental results showed that the reaction rate over the three catalysts was dependent on the hydrogen and naphthalene concentration. Consequently, models 11 and 14 were excluded before regression for not showing this effect.

The experimental data were regressed with the other 12 models. Initially, the data fitting was carried out with the rate expressions including lumped parameters, for example, in model 1, $k_3 b_N b_H^{1/2}$ was treated as one single parameter, i.e., k_3'. However, it was observed that, in general, maintaining the parameters lumped led to highly correlation coefficients between parameters. It was further decided to unlump the parameters in the rate expression. By doing so, it was observed that the correlation matrix improved quite significantly. The results presented were obtained by regression of the rate expressions with unlumped parameters

3.2.1. $NiMo/Al_2O_3$ catalyst

The two sets of experiments with different concentrations of naphthalene and hydrogen at 523.15 K (intrinsic regime) and 573.15 K (pore diffusion regime) were regressed.

3.2.1.1. The Intrinsic regime. An attempt in regressing the complete set of results, i.e., the experimental rates of reaction obtained by varying both hydrogen and naphthalene concentrations at 523.15 K, was made. However, this regression did not produce realistic results and the parameters were estimated by regressing only the data set where naphthalene concentration was varied at 523.15 K and 30×10^5 Pa and only these regression results are presented.

The regression of models 2, 9 and 10 only produced a negative estimate of the parameters, which is not physically meaningful; moreover, model 13 failed to converge. Consequently, these latter models were excluded from further analysis. From the regression results, it was observed that all the other models fitted the results with positive estimates for the parameters. The rate parameters along with their 95% confidence interval, SSR_{min} and the regression coefficients (Rc) are given in Table 1.

For the purpose of model discrimination, a comparison of the regression coefficient for the models and confidence interval, obtained for each estimated parameter, was initially performed. As it can be observed from the results, model 12 exhibited a very low correlation coefficient compared with the other models and therefore was discarded as a good representation of the experimental data. All other models had a very similar correlation coefficient and minimized sum of the squares of the residuals. Analysing the confidence interval of each estimated parameter, models 4–8 had two parameters with a negative confidence interval, thus making them physically not meaningful. These latter models were therefore discarded.

The final rival models are model 1, where surface reaction is the limiting step (step III) with hydrogen adsorbing atomically, and model 3, where the surface reaction is also the limiting step (step III) but hydrogen is considered to adsorb molecularly. Models 1 and 3 exhibited both a negative confidence interval for the adsorption constant of hydrogen. The estimated value of the adsorption constant for naphthalene exhibited a higher confidence interval with model 1 than with model 3. However, the observed difference was not that significant. At this point and in order to discriminate between these two models the one

Table 1
Estimated parameters, regression coefficient (Rc) and minimum sum of square of residuals ($SSR)_{min}$ for the naphthalene hydrogenation at 523.15 K over the presulphided $NiMo/Al_2O_3$ catalyst

L–H rate equations	k_1, k_3 or k_4 (depending on the equation)	b_H or b_{H2} ($m^3\ mol_{H2,H}^{-1}$)	b_N ($m^3\ mol_N^{-1}$)	K_3	Rc	$(SSR)_{min}$	Model
$r_3 = \frac{k_3 b_N b_H^{1/2} C_N C_{H_2}}{(1+b_H^{1/4} C_{H_2}^{1/2} + b_N C_N)^3}$	$2.50 \times 10^{-1} \pm 1.00 \times 10^{-5}$	$7.57 \times 10^{-6} \pm 1.48 \times 10^{-5}$	$9.89 \times 10^{-4} \pm 7.64 \times 10^{-4}$	–	0.969	2.20×10^{-7}	1
$r_3 = \frac{k_3 b_N b_{H_2}^{1/2} C_N C_{H_2}}{(1+b_{H_2}^{1/2} C_{H_2} + b_N C_N)^2}$	$4.97 \times 10^{-2} \pm 3.09 \times 10^{-5}$	$4.01 \times 10^{-5} \pm 1.02 \times 10^{-4}$	$1.93 \times 10^{-3} \pm 7.86 \times 10^{-4}$	–	0.969	2.20×10^{-7}	3
$r_4 = \frac{k_4 b_{H_2} b_N K_3 C_N C_{H_2}^2}{(1+b_{H_2}^{1/2} C_{H_2} + b_N C_N + K_3 b_N b_{H_2}^{1/2} C_N C_{H_2})^2}$	$2.19 \times 10^{-1} \pm 1.00 \times 10^{-6}$	$8.65 \times 10^{-6} \pm 1.37 \times 10^{-5}$	$9.06 \times 10^{-4} \pm 1.57 \times 10^{-3}$	1.17 ± 0	0.969	2.20×10^{-7}	4
$r_3 = \frac{k_3 b_N b_H^{1/2} C_N C_{H_2}}{(1+b_H^{1/4} C_{H_2}^{1/2})^2 (1+b_N C_N)}$	$2.58 \times 10^{-2} \pm 9.95 \times 10^{-5}$	$3.30 \times 10^{-4} \pm 1.44 \times 10^{-3}$	$2.43 \times 10^{-3} \pm 3.14 \times 10^{-3}$	–	0.968	2.21×10^{-7}	5
$r_4 = \frac{k_4 b_H b_N K_3 C_N C_{H_2}^2}{(1+b_H^{1/4} C_{H_2}^{1/2})^2 (1+b_N C_N + K_3 b_N b_H^{1/2} C_N C_{H_2})}$	$4.53 \times 10^{-2} \pm 1.29 \times 10^{-4}$	$6.43 \times 10^{-4} \pm 2.08 \times 10^{-3}$	$1.20 \times 10^{-3} \pm 3.54 \times 10^{-3}$	$2.52 \times 10^{-1} \pm 3.00 \times 10^{-6}$	0.968	2.21×10^{-7}	6
$r_3 = \frac{k_3 b_N b_{H_2}^{1/2} C_N C_{H_2}}{(1+b_{H_2}^{1/2} C_{H_2})(1+b_N C_N)}$	$1.93 \times 10^{-2} \pm 1.90 \times 10^{-6}$	$4.96 \times 10^{-5} \pm 1.71 \times 10^{-4}$	$2.43 \times 10^{-4} \pm 3.14 \times 10^{-3}$	–	0.968	2.21×10^{-7}	7
$r_4 = \frac{k_4 b_{H_2} b_N K_3 C_N C_{H_2}^2}{(1+b_{H_2}^{1/2} C_{H_2})(1+b_N C_N + K_3 b_N b_{H_2}^{1/2} C_N C_{H_2})}$	$1.52 \times 10^{-2} \pm 1.98 \times 10^{-2}$	$2.03 \times 10^{-1} \pm 2.43 \times 10^{-4}$	$7.67 \times 10^{-4} \pm 1.70 \times 10^{-3}$	$2.99 \times 10^{-2} \pm 3.15 \times 10^{-3}$	0.968	2.21×10^{-7}	8
$r_1 = \frac{k_1 C_N}{(1+b_H^{1/4} C_{H_2}^{1/2})}$	$3.80 \times 10^{-4} \pm 6.69 \times 10^{-5}$	13.14 ± 0	–	–	0.835	1.16×10^{-6}	12

Table 2
Correlation matrices derived from rival models 1 and 3 at 523.15 K for the $NiMo/Al_2O_3$ catalyst

Model	$r_{w,N}^{obs}(\text{mol kg}_{NiMo}^{-1}\,s^{-1})$	σ_{ij}
1	$r_3 = \frac{k_3 b_N b_H^{1/2} C_N C_{H_2}}{(1+b_H^{1/4} C_{H_2}^{1/2} + b_N C_N)^3}$	$\begin{pmatrix} 1 & -0.977 & 1.00 \\ -0.977 & 1 & -0.977 \\ 1.00 & -0.977 & 1 \end{pmatrix}$
3	$r_3 = \frac{k_3 b_N b_{H_2}^{1/2} C_N C_{H_2}}{(1+b_{H_2}^{1/2} C_{H_2} + b_N C_N)^2}$	$\begin{pmatrix} 1 & -0.913 & 0.999 \\ -0.913 & 1 & -0.915 \\ 0.999 & -0.915 & 1 \end{pmatrix}$

that better described the kinetic data, another criterion was applied. This criterion was based on the analysis of the correlation coefficients between the parameters obtained with each model [20–23].

The correlation matrix obtained by the Mathematica™ 5 program, for the two left plausible models, is given in Table 2. The correlation coefficient between parameter i and parameter j is indicated by σ_{ij} in the correlation matrix. k_3 (or k_4), b_{H_2} (b_H) and b_N are parameters 1, 2 and 3, respectively. It is observed from this table that k_3, b_{H_2} (b_H) are highly correlated in both models. However, as pointed out in previous works, highly correlated estimates may be obtained with L–H-type models [24]. The high correlation observed between the parameters does not necessarily mean that the observed values are not reliable, but their correlation is a consequence of their position in the equation since they are multiplying by each other. Nevertheless, model 3 produced the lowest correlation coefficients between parameters. Therefore, the best fit, in a strictly mathematical sense, was obtained by this model, where hydrogen is assumed to adsorb molecularly on the surface of the catalyst. A comparison between the model and the experimental data is shown in Fig. 1.

3.2.1.2. Pore diffusion regime. The parameter estimation was first carried out by regressing only the data where naphthalene concentration was varied at 573.15 K and 30×10^5 Pa. However, in this case, it was not possible to estimate the adsorption parameter for hydrogen accurately, and unrealistic values were obtained. This was improved by regressing simultaneously this latter data set with the data set where hydrogen partial pressure was varied from (10–30) $\times 10^5$ Pa at 573.15 K. Only the results from this simultaneous regression are presented.

Model 2 failed to converge, whereas models 9, 10, 12 and 13 only converged to a negative solution and therefore were excluded as representing the data. The data regression with the other models produced a positive result and a simultaneous and careful analysis on the 95% confidence interval, SSR_{min}, Rc and correlation matrix had to be taken in order to discriminate the best among them. The results are presented in Table 3. For the correlation matrix k_3 (or k_4) is parameter 1, b_{H_2} (b_H) is parameter 2, b_N parameter 3 and K_3 parameter 4.

Analysing the regression coefficient for each model, it can be noticed that all models exhibited quite similar values. An insight into the size of the confidence interval was therefore taken. Although models 4 and 8 presented high values for Rc, an unavoidable large confidence interval was observed for the estimates of the parameters. In addition, the observed correlation coefficients were very high for all the estimated parameters and therefore, these two models were discarded.

In the case of model 6, it was noticed that it presented a quite high estimate of b_H. In addition, this estimate was higher than the one for b_N. Since naphthalene adsorbs stronger than hydrogen on the surface of the catalyst, due to its delocalised electrons, its adsorption constant should be higher than the one for hydrogen and therefore, this model was discarded. Moreover, all the correlation coefficients were close to one, which reinforces its dismissal. Models 1 and 5 presented negative confidence intervals for two (k_3 and b_H) out of the three estimated parameters, whereas models 3 and 7 only presented a negative confidence interval for b_H. Therefore, these latter models are considered a better representation of the experimental data than the former models. The final rival models are the models that assume that step III (first addition of

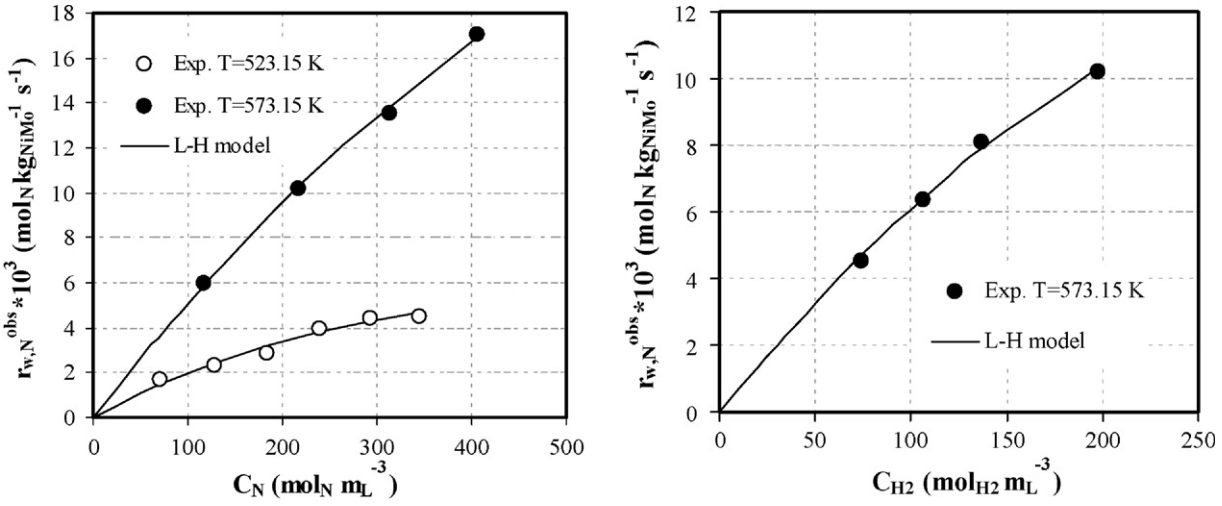

Fig. 1. Experimental versus L–H model results (model 3): effect of naphthalene concentration ($P_{H_2} = 30 \times 10^5$ Pa) and hydrogen concentration (325 $mol_N\,m^{-3}$) on the initial HYD rate of naphthalene over the presulphided $NiMo/Al_2O_3$ catalyst.

Table 3
Estimated parameters, correlation matrix, regression coefficient (Rc) and minimum sum of square of residuals $(SSR)_{min}$ for the naphthalene hydrogenation at 573.15 K over the presulphided $NiMo/Al_2O_3$ catalyst

L–H rate equations	k_3 or k_4 (depending on the equation)	b_H or $b_{H2}(m^3\,mol_{H2}^{-1})$	$b_N(m^3\,mol_N^{-1})$	K_3	Rc	$(SSR)_{min}$	Model
$r_3 = 0.67\frac{k_3 b_N b_H^{1/2} C_N C_{H_2}}{(1+b_H^{1/4} C_{H_2}^{1/2}+b_N C_N)^3}$	14.11 ± 16.82	$2.98\times10^{-8} \pm 8.99\times10^{-8}$	$2.86\times10^{-4} \pm 1.35\times10^{-4}$	–	0.998	2.56×10^{-7}	1
		Correlation matrix $\begin{pmatrix} 1 & -0.951 & -0.155 \\ -0.951 & 1 & -0.158 \\ -0.155 & -0.158 & 1 \end{pmatrix}$					
$r_3 = 0.67\frac{k_3 b_N b_{H_2}^{1/2} C_N C_{H_2}}{(1+b_{H_2}^{1/2} C_{H_2}+b_N C_N)^2}$	1.56 ± 0.86	$7.19\times10^{-7} \pm 9.29\times10^{-7}$	$4.34\times10^{-4} \pm 1.97\times10^{-4}$		0.998	2.10×10^{-7}	3
		Correlation matrix $\begin{pmatrix} 1 & -0.769 & -0.486 \\ -0.769 & 1 & -0.184 \\ -0.486 & -0.184 & 1 \end{pmatrix}$					
$r_4 = 0.67\frac{k_4 b_{H_2} b_N K_3 C_N C_{H_2}^2}{(1+b_{H_2}^{1/2} C_{H_2}+b_N C_N+K_3 b_N b_{H_2}^{1/2} C_N C_{H_2})^2}$	$4.67 \pm 5.12\times10^{3}$	$1.96\times10^{-4} \pm 1.17\times10^{-2}$	$1.26\times10^{-3} \pm 0.126$	$2.58\times10^{-2} \pm 31.30$	0.999	1.20×10^{-7}	4
		Correlation matrix $\begin{pmatrix} 1 & 0.999 & 0.999 & -1.0 \\ 0.999 & 1 & 0.999 & -0.999 \\ 0.999 & 0.999 & 1 & -0.999 \\ -1.0 & -0.999 & -0.999 & 1 \end{pmatrix}$					
$r_3 = 0.67\frac{k_3 b_N b_H^{1/2} C_N C_{H_2}}{(1+b_H^{1/4} C_{H_2}^{1/2})^2 (1+b_N C_N)}$	2.06 ± 2.37	$1.58\times10^{-7} \pm 5.02\times10^{-7}$	$8.52\times10^{-4} \pm 4.79\times10^{-4}$	–	0.998	2.42×10^{-7}	5
		Correlation matrix $\begin{pmatrix} 1 & -0.934 & 0.052 \\ -0.934 & 1 & -0.404 \\ 0.052 & -0.404 & 1 \end{pmatrix}$					
$r_4 = 0.67\frac{k_4 b_H b_N K_3 C_N C_{H_2}^2}{(1+b_H^{1/4} C_{H_2}^{1/2})^2 (1+b_N C_N+K_3 b_N b_H^{1/2} C_N C_{H_2})}$	$8.64\times10^{-2} \pm 3.80\times10^{-2}$	$4.45\times10^{4} \pm 0$	$5.90\times10^{-11} \pm 3.34\times10^{-11}$	420.4 ± 0	0.997	3.36×10^{-7}	6
		Correlation matrix $\begin{pmatrix} 1 & 1.0 & -0.996 & 1.0 \\ 1.0 & 1 & -0.996 & 1.0 \\ -0.996 & -0.996 & 1 & -0.996 \\ 1.0 & 1.0 & -0.996 & 1 \end{pmatrix}$					
$r_3 = 0.67\frac{k_3 b_N b_{H_2}^{1/2} C_N C_{H_2}}{(1+b_{H_2}^{1/2} C_{H_2})(1+b_N C_N)}$	0.392 ± 0.212	$2.99\times10^{-6} \pm 4.35\text{x}10^{-6}$	$8.42\times10^{-4} \pm 4.40\times10^{-4}$	–	0.998	2.05×10^{-7}	7
		Correlation matrix $\begin{pmatrix} 1 & -0.711 & -0.348 \\ -0.711 & 1 & -0.411 \\ -0.348 & -0.411 & 1 \end{pmatrix}$					
$r_4 = 0.67\frac{k_4 b_{H_2} b_N K_3 C_N C_{H_2}^2}{(1+b_{H_2}^{1/2} C_{H_2})(1+b_N C_N+K_3 b_N b_{H_2}^{1/2} C_N C_{H_2})}$	$8.63\times10^{-2} \pm 0.116$	$1.13\times10^{3} \pm 3.29\times10^{3}$	$5.47\times10^{-8} \pm 1.68\times10^{-3}$	$2.81 \pm 8.60\times10^{4}$	0.997	3.22×10^{-7}	8
		Correlation matrix $\begin{pmatrix} 1 & -0.946 & 0.946 & -0.946 \\ -0.946 & 1 & -1.0 & 1.0 \\ 0.946 & -1.0 & 1 & -1.0 \\ -0.946 & 1.0 & -1.0 & 1 \end{pmatrix}$					

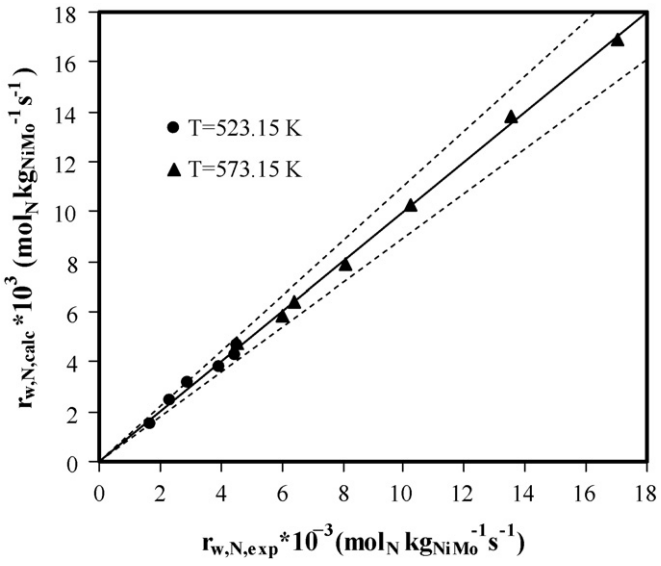

Fig. 2. Parity plot of the experimental results versus L–H model results (model 3) obtained over the presulphided $NiMo/Al_2O_3$ catalyst at 523.15 and 573.15 K, including the 95% confidence interval.

hydrogen) is the rate limiting step, hydrogen is adsorbed molecularly on the catalyst surface and that hydrogen and naphthalene both compete for the same active sites (model 3) or adsorb on different catalytic sites (model 7). These two models exhibited very similar statistical features. However, an insight into the size of the confidence intervals reveals that confidence interval of b_{H_2} was slightly smaller in model 3 than in model 7 and was negative in both the models. Therefore, the former model, where it is assumed that hydrogen and naphthalene adsorb on the same catalytic sites, represents, in a mathematical sense, a better fit of the experimental data. Although b_{H_2} exhibited a slightly negative confidence the estimated value can be considered reliable, since a low correlation coefficient between this parameter and the others was obtained. The highest correlation coefficient observed was with the parameter k_3 and had a value of -0.769, which is considered a low value. A comparison between the model and the experimental data is shown in Fig. 1 for the effect of hydrogen concentration and naphthalene concentration.

The same mechanism was observed for both intrinsic and pore diffusion regimes during the naphthalene HYD over the $NiMo/Al_2O_3$. The goodness of the L–H model fit (model 3) to the experimental data, for the two regimes, is illustrated in the parity plot presented in Fig. 2. The 95% confidence interval for a normal distribution, i.e., $\pm 1.96 \times S_{td}$, where S_{td} is the standard deviation and was found to be equal to 5.4% for all the regressed experimental data, is also presented. The first surface addition of hydrogen (step III) was the limiting step, which is intuitively satisfactory, as one would anticipate that the largest activation barrier should be that for breaking the resonance of the aromatic ring. In addition, the best fit of the data was given by assuming a non-dissociative adsorption of hydrogen. However, whether hydrogen can adsorb molecularly on the surface of the catalyst is still a controversial issue. From a chemical point of view, the atomic adsorption of hydrogen on the surface of the catalyst is more probable than the molecular adsorption. However, according to Smeds et al. [15], the fact that the addition of two hydrogen atoms to the aromatic molecule is a three-body process cannot rule out the possibility of pairwise addition of hydrogen molecules, since the surface species are not expected to be as mobile as in the fluid phase. Molecular adsorption of hydrogen on the surface of the catalyst has been reported in the literature for the HYD benzene [18]. In general, a dissociative adsorption of hydrogen during naphthalene HYD was reported [25–27]. According to Lindfords and Salmi [28], the character of hydrogen adsorption has only a minor effect on the rate of the equation and conclusions of the true form of hydrogen adsorption based solely on the experimentally measured HYD kinetics is a very difficult task. In agreement with this observation, Toppinen et al. [16] reported it to be impossible to discriminate between molecular and atomic adsorption based on their benzene HYD data over a Ni catalyst. The results also showed that the adsorption was competitive, i.e., naphthalene and hydrogen molecules (or atoms) adsorbed on the same sites. Both competitive and non-competitive adsorptions of hydrogen and naphthalene during naphthalene HYD have been reported in the literature [26,27]. Smeds et al. [15] studied the HYD of ethylbenezene over a Ni/Al_2O_3 catalyst and stated that the true nature of coadsorption of the reactants lies somewhere in between competitive and non-competitive adsorption. These authors also believe that the larger size of the aromatic molecules cannot rule out completely the competitive adsorption of the much smaller hydrogen atoms or molecules and, therefore, the discrimination between competitive and non-competitive adsorption is revealed to be a difficult task.

A summary of the estimates of the kinetic constants found by the L–H model is given in Table 4. Comparing the estimated parameters from the L–H model for the intrinsic and pore diffusion regimes, it can be observed that the adsorption constants of naphthalene and hydrogen, and therefore the catalytic surface coverage by these reactants, decreased with increased temperature, as expected. This effect was more pronounced in the case of the hydrogen adsorption constant,

Table 4
Summary of the parameters estimated using the best fitting model for the naphthalene hydrogenation over the presulphided $NiMo/Al_2O_3$ catalyst at 523.15 and 573.15 K

T (K)	P_{H_2} ($\times 10^{-5}$ Pa)	C_N ($mol_N\ m^{-3}$)	k_3 [a]	b_{H2} ($m^3\ mol_{H2}^{-1}$)	b_N ($m^3\ mol_N^{-1}$)	L–H model
523.15	30	96–470	4.97×10^{-2}	4.01×10^{-5}	1.93×10^{-3}	Model 3
573.15	10–30	174–609	1.56	7.19×10^{-7}	4.34×10^{-4}	

[a] See mechanism 3 rate expression.

Table 5
Estimated parameters, correlation matrix, regression coefficient (Rc) and minimum sum of square of residuals $(SSR)_{min}$ for the naphthalene hydrogenation at 373.15 K over the Ni/Al_2O_3 catalyst

L–H rate equations	k_3 or k_4 (depending on the equation)	b_H or $b_{H2}(m^3\,mol_{H2}^{-1})$	$b_N(m^3\,mol_N^{-1})$	K_3	Rc	$(SSR)_{min}$	Model
$r_3 = 0.14\frac{k_3 b_N b_H^{1/2} C_N C_{H_2}}{(1+b_H^{1/4} C_{H_2}^{1/2}+b_N C_N)^3}$	3.33 ± 12.46	$5.76 \times 10^{-4} \pm 1.70 \times 10^{-3}$	$2.39 \times 10^{-3} \pm 1.76 \times 10^{-3}$	–	0.923	1.01×10^{-5}	1
$r_3 = 0.14\frac{k_3 b_N b_{H_2}^{1/2} C_N C_{H_2}}{(1+b_{H_2}^{1/2} C_{H_2}+b_N C_N)^2}$	1.24 ± 0.533	$2.63 \times 10^{-4} \pm 3.47 \times 10^{-4}$	$3.67 \times 10^{-3} \pm 2.56 \times 10^{-3}$		0.940	7.95×10^{-6}	3
			Correlation matrix $\begin{pmatrix} 1 & -0.939 & -0.926 \\ -0.939 & 1 & 0.787 \\ -0.926 & 0.787 & 1 \end{pmatrix}$				
$r_4 = 0.14\frac{k_4 b_{H_2} b_N K_3 C_N C_{H_2}^2}{(1+b_{H_2}^{1/2} C_{H_2}+b_N C_N+K_3 b_N b_{H_2}^{1/2} C_N C_{H_2})^2}$	0.815 ± 0.209	$2.44 \times 10^{-3} \pm 3.82 \times 10^{-3}$	$2.94 \times 10^{-4} \pm 2.05 \times 10^{-4}$	$9.10 \pm 1.50 \times 10^{-4}$	0.937	8.35×10^{-6}	4
$r_3 = 0.14\frac{k_3 b_N b_H^{1/2} C_N C_{H_2}}{(1+b_H^{1/4} C_{H_2}^{1/2})^2 (1+b_N C_N)}$	0.524 ± 0.271	$1.45 \times 10^{-3} \pm 3.38 \times 10^{-3}$	$8.40 \times 10^{-3} \pm 6.06 \times 10^{-3}$	–	0.958	5.52×10^{-6}	5
			Correlation matrix $\begin{pmatrix} 1 & -0.899 & -0.396 \\ -0.899 & 1 & -0.030 \\ -0.396 & -0.030 & 1 \end{pmatrix}$				
$r_3 = 0.14\frac{k_3 b_N b_{H_2}^{1/2} C_N C_{H_2}}{(1+b_{H_2}^{1/2} C_{H_2})(1+b_N C_N)}$	$0.310 \pm 9.46 \times 10^{-2}$	$7.64 \times 10^{-4} \pm 8.86 \times 10^{-4}$	$8.17 \times 10^{-3} \pm 5.44 \times 10^{-3}$	–	0.964	4.82×10^{-6}	7
			Correlation matrix $\begin{pmatrix} 1 & -0.718 & -0.653 \\ -0.718 & 1 & -0.028 \\ -0.653 & -0.028 & 1 \end{pmatrix}$				

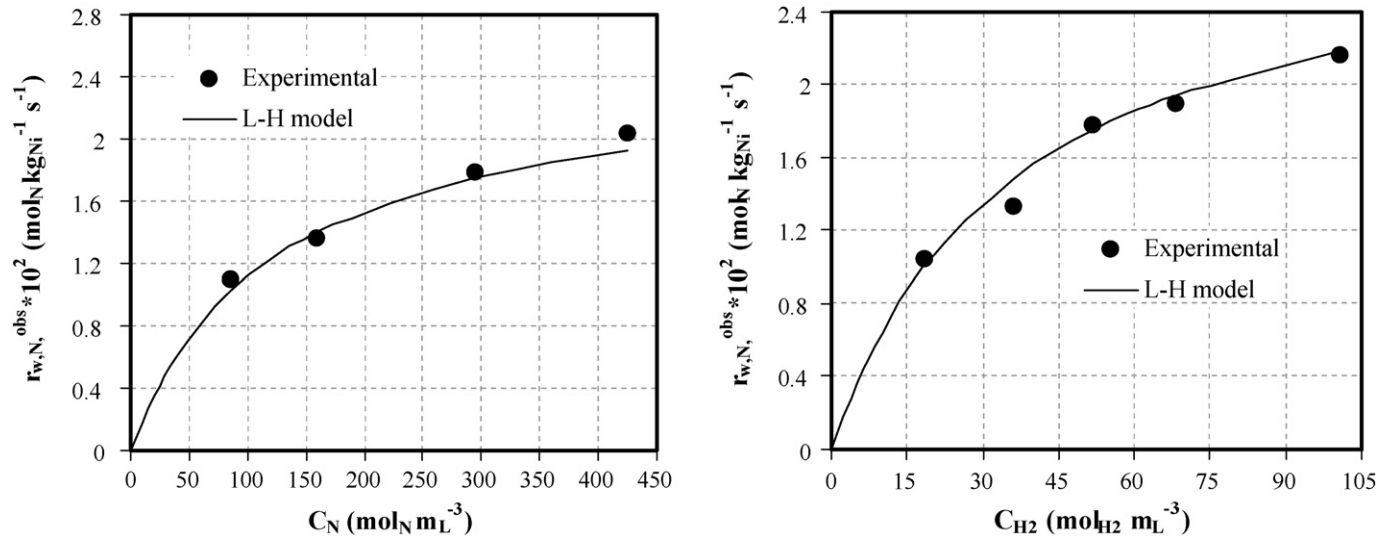

Fig. 3. Experimental versus L–H model results (model 7): effect of naphthalene concentration ($P_{H_2} = 15 \times 10^5$ Pa) and hydrogen concentration (325 $mol_N\ m_L^{-3}$) on the initial HYD rate of naphthalene over the prereduced Ni/Al_2O_3 catalyst at 373.15 K.

i.e., the hydrogen adsorption constant decreased more with temperature than the naphthalene adsorption constant. In both regimes, the naphthalene adsorption constant was found to be clearly higher than the hydrogen one, indicating that naphthalene molecules adsorbed more strongly on the surface of the catalyst than the hydrogen atoms or molecules, as noted before. The rate constant for step III, i.e., k_3, was found to increase with increased temperature, as it was also expected.

3.2.2. Ni/Al_2O_3 catalyst

The parameter estimation was first carried out by regressing only the data where naphthalene concentration was varied at 373.15 K and 15×10^5 Pa. However, in this case, it was not possible to estimate the adsorption parameter for hydrogen accurately, and unrealistic values were obtained. This was improved by regressing simultaneously this latter data set with the data set where hydrogen partial pressure was varied from $(5–30) \times 10^5$ Pa at 573.15 K. Only the results from this simultaneous regression are presented.

It was observed that models 6, 8, 9, 10, 12 and 13 generated at least one negative estimate for one of the parameters and were therefore excluded from further analysis. Model 2 was also excluded because it failed to converge to any solution. All the other models converged and produced positive estimates. The parameters and their 95% confidence interval, along with the SSR_{min} and Rc, are given in Table 5.

Comparing the Rc values obtained from each model presented in Table 5, it can be observed that model 1 exhibited the lowest Rc and consequently the highest $(SSR)_{min}$ of all the models and therefore was excluded as being the best representation of the experimental data. Model 4 produced a higher estimate of b_{H_2} than b_N. Since naphthalene adsorbs more strongly than hydrogen on the surface of the catalyst, for the reasons pointed out before, it is expected the b_N value to be higher than the b_{H_2} and therefore, this model was discarded. Models 3, 5 and 7 fitted the data well. From these three models, model 3 presented the lowest Rc value, nevertheless it was decided to not discard it based only on this analysis and a careful insight into the correlation matrices of these three models was taken. The correlation matrix for these models is also presented in Table 5. In the correlation matrix k_3, b_{H_2} (b_H) and b_N are parameters 1, 2 and 3, respectively.

Comparing the correlation matrices from these three models, it can be observed that model 3 presented the highest correlation coefficients between parameters and this, coupled with the fact that it exhibited the lowest Rc value, leads to its dismissal. The final plausible models are model 5, where non-competitive, dissociative adsorption of hydrogen is assumed and model 7, where non-competitive, molecular adsorption of hydrogen is assumed. Both models presented similar values of

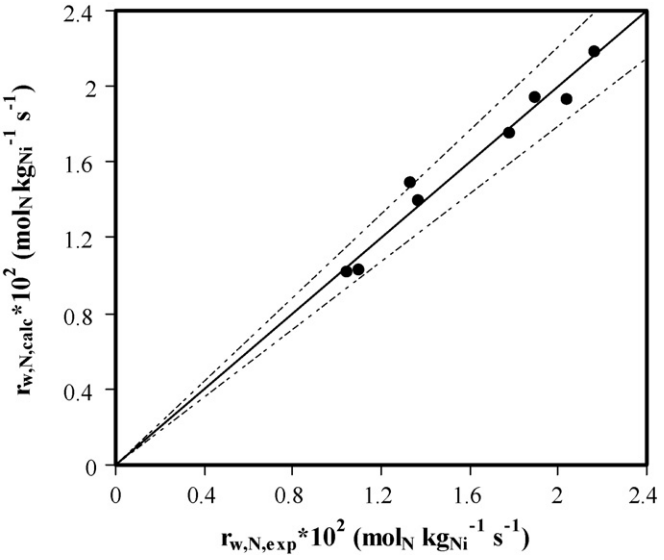

Fig. 4. Parity plot of the experimental results versus L–H model results (model 7) obtained over the prereduced Ni/Al_2O_3 catalyst at 373.15 K, including the 95% confidence interval.

Table 6
Estimated parameters, correlation matrix, regression coefficient (Rc) and minimum sum of square of residuals $(SSR)_{min}$ for the naphthalene hydrogenation at 373.15 K over the Ru/Al_2O_3 catalyst

L–H rate equations	k_3 or k_4 (depend on the equation)	b_H or $b_{H2}(m^3\,mol_{H2}^{-1})$	$b_N(m^3\,mol_N^{-1})$	K_3	Rc	$(SSR)_{min}$	Model
$r_3 = 0.15\frac{k_3 b_N b_H^{1/2} C_N C_{H_2}}{(1+b_H^{1/4} C_{H_2}^{1/2}+b_N C_N)^3}$	19.13 ± 7.97	$3.40 \times 10^{-3} \pm 7.47 \times 10^{-3}$	$3.12 \times 10^{-3} \pm 1.55 \times 10^{-3}$	–	0.935	5.32×10^{-4}	1
			Correlation matrix $\begin{pmatrix} 1 & -0.985 & -0.924 \\ -0.985 & 1 & 0.879 \\ -0.924 & 0.879 & 1 \end{pmatrix}$				
$r_3 = 0.15\frac{k_3 b_N b_{H_2}^{1/2} C_N C_{H_2}}{(1+b_{H_2}^{1/2} C_{H_2}+b_N C_N)^2}$	8.07 ± 2.43	$6.78 \times 10^{-4} \pm 8.60 \times 10^{-4}$	$5.04 \times 10^{-3} \pm 3.02 \times 10^{-3}$		0.918	6.65×10^{-4}	3
$r_3 = 0.15\frac{k_3 b_N b_H^{1/2} C_N C_{H_2}}{(1+b_H^{1/4} C_{H_2}^{1/2})^2 (1+b_N C_N)}$	2.88 ± 1.02	$1.14 \times 10^{-2} \pm 2.52 \times 10^{-2}$	$9.68 \times 10^{-3} \pm 5.12 \times 10^{-3}$	–	0.950	4.05×10^{-4}	5
			Correlation matrix $\begin{pmatrix} 1 & -0.914 & -0.388 \\ -0.914 & 1 & 0.002 \\ -0.388 & 0.002 & 1 \end{pmatrix}$				
$r_4 = 0.15\frac{k_4 b_H b_N K_3 C_N C_{H_2}^2}{(1+b_H^{1/4} C_{H_2}^{1/2})^2 (1+b_N C_N+K_3 b_N b_H^{1/2} C_N C_{H_2})}$	1.48 ± 3.79	$1.71 \times 10^4 \pm 2.49 \times 10^7$	$4.64 \times 10^{-6} \pm 5.82 \times 10^{-2}$	$0.297 \pm 3.94 \times 10^3$	0.943	4.62×10^{-4}	6
$r_3 = 0.15\frac{k_3 b_N b_{H_2}^{1/2} C_N C_{H_2}}{(1+b_{H_2}^{1/2} C_{H_2})(1+b_N C_N)}$	1.98 ± 0.456	$2.45 \times 10^{-3} \pm 3.08\text{x}10^{-3}$	$9.69 \times 10^{-3} \pm 5.47 \times 10^{-3}$	–	0.942	4.69×10^{-4}	7
			Correlation matrix $\begin{pmatrix} 1 & -0.744 & -0.634 \\ -0.744 & 1 & 0.0003 \\ -0.634 & 0.0003 & 1 \end{pmatrix}$				
$r_4 = 0.15\frac{k_4 b_{H_2} b_N K_3 C_N C_{H_2}^2}{(1+b_{H_2}^{1/2} C_{H_2})(1+b_N C_N+K_3 b_N b_{H_2}^{1/2} C_N C_{H_2})}$	1.47 ± 0.298	$1.90 \times 10^5 \pm 0$	$1.91 \times 10^{-4} \pm 2.50 \times 10^{-3}$	$2.13 \times 10^{-3} \pm 2.76 \times 10^{-2}$	0.943	4.60×10^{-4}	8

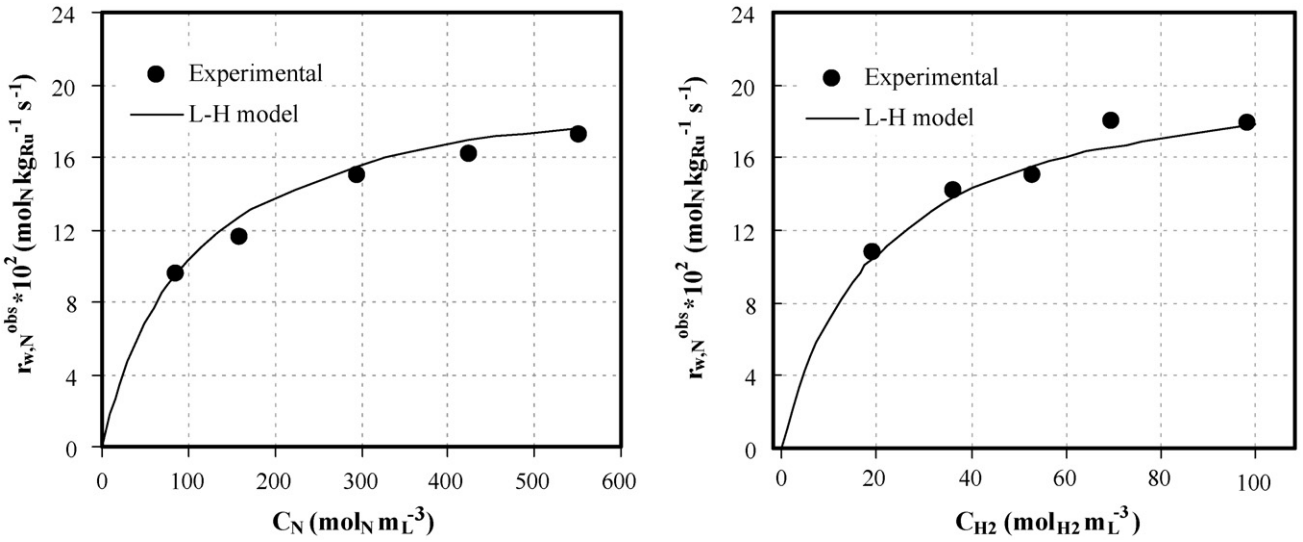

Fig. 5. Experimental versus L–H model results (model 7): effect of naphthalene concentration ($P_{H_2} = 15 \times 10^5$ Pa) and hydrogen concentration (325 mol$_N$ m$_L^{-3}$) on the initial HYD rate of naphthalene over the prereduced Ru/Al_2O_3 catalyst at 373.15 K.

Rc and $(SSR)_{min}$. Analysing the correlation matrices it can be noticed that model 7 exhibited a lower correlation coefficient between k_3 and b_{H_2} than model 5. On the other hand, the former model presented a higher correlation coefficient between k_3 and b_N, making evident the difficulty in discriminating the best between these two models. However, model 7 produced narrower confidence intervals for the estimates than model 5, especially for b_{H_2} and it can be concluded that it fitted better the experimental data than model 5. Although a slightly negative confidence interval was obtained for b_{H_2}, its estimate can be considered reliable since the correlation coefficients between this parameter and the other parameters were low. This means that it is unlikely that there is another solution that fits the experimental data equally well. The highest correlation coefficient found was with k_3 and had a value of -0.718. The good agreement between experimental and predicted data by model 7 is illustrated in Fig. 3 and in the parity plot presented in Fig. 4, which includes the 95% confidence interval for a normal distribution of the data ($S_{td} = 5.3\%$, for all regressed experimental data).

The hydrogen adsorption constant was found to be 1 order of magnitude lower than the adsorption constant for naphthalene. This is not surprising, as noted before, since naphthalene, as an aromatic compound, is expected to adsorb more strongly on the catalyst surface than hydrogen. The adsorption constant values for hydrogen and naphthalene found in this work, 7.64×10^{-4} and 8.17×10^{-3} m^3 mol^{-1}, respectively, are similar to the ones reported by Lylykangas et al. [25] over a Ni/Al_2O_3 catalyst between 353.15 and 413.15 K (3.7×10^{-3} and 7.8×10^{-3} m^3 mol^{-1}, respectively). However, they differ from the ones reported by Rautanen et al. [26].

In summary, the surface reaction with the first addition of hydrogen (step III) was found to control the naphthalene HYD over the Ni/Al_2O_3 catalyst at 373.15 K. The best fit found for the experimental data was by assuming that hydrogen adsorbs molecularly on the surface, which can be controversial from a chemical point of view, as discussed before. In addition, the results show that hydrogen is adsorbed on different catalytic sites than naphthalene.

3.3. Ru/Al_2O_3 catalyst

The two sets of experiments with different concentrations of naphthalene and hydrogen at 373.15 K were regressed simultaneously. From the regression results, it was observed that models 4, 9, 10, 12, and 13 only converged to a negative estimate of one or more parameters, which is not physically meaningful. In addition, model 2 failed to converge. These models were therefore excluded from further analysis. The

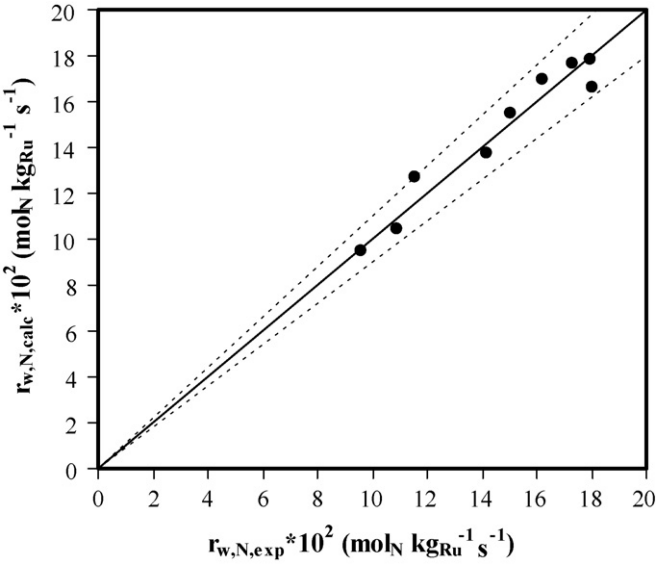

Fig. 6. Parity plot of the experimental results versus L–H model results (model 7) obtained over the prereduced Ru/Al_2O_3 catalyst at 373.15 K, including the 95% confidence interval.

Table 7
Summary of the parameters obtained via experimental data regression for the naphtalene hydrogenation over the presulphided NiMo and prereduced Ni and Ru/Al_2O_3 catalysts

Catalyst	T (K)	P_{H_2} ($\times 10^{-5}$ Pa)	C_N ($mol_N\ m^{-3}$)	k_3 ([a])	$b_{H2}(m_L^3\ mol_{H2}^{-1})$	$b_N(m_L^3\ mol_N^{-1})$	L–H model
$NiMo/Al_2O_3$	573.15	10–30	174–609	1.56	7.19×10^{-7}	4.34×10^{-4}	Competitive molecular adsorption of H_2
	523.15	30	96–470	4.97×10^{-2}	4.01×10^{-5}	1.93×10^{-3}	Competitive molecular adsorption of H_2
Ni/Al_2O_3	373.15	5–30	94–470	0.31	7.64×10^{-4}	8.17×10^{-3}	Non-competitive molecular adsorption of H_2
Ru/Al_2O_3	373.15	5–30	94–610	1.98	2.45×10^{-3}	9.69×10^{-3}	Non-competitive molecular adsorption of H_2

[a] See rate expressions.

other models converged to positive estimates of the parameters and the values along with their 95% confidence interval $(SSR)_{min}$ and Rc values, are collected in Table 6.

As the table shows, the Rc obtained from model 3 presented the lowest value and therefore the highest $(SSR)_{min}$ of all the models. Based on this low Rc, this model was excluded from further analysis, because all the others fitted better the experimental data. Models 6 and 8 produced an unrealistically high estimate for b_H (b_{H_2}) and moreover, this estimate was considerably higher than the estimate found for b_N. Therefore, these two latter models were discarded as being a good representation of the experimental data. Models 1, 5 and 7 were found to fit well the data. From these three models, model 1 presented the lowest Rc and model 5 the highest, but the difference between them was not considerable. Therefore, the discrimination was not based solely on this fact and a careful insight into the size of the confidence intervals and the correlation matrices was carried out in order to discriminate the one that fitted best the experimental data. The correlation matrix for these models is presented in Table 6. As before, k_3, b_{H_2} (b_H) and b_N are parameters 1, 2 and 3, respectively, in the correlation matrix.

Regarding correlation coefficients obtained with these three models, it can be observed that model 1 presents the highest correlation between parameters and hence it was discarded. Its removal was supported by its low regression coefficient. After this analysis, the plausible models are then model 5, where non-competitive, dissociative adsorption of hydrogen is assumed and model 7, where non-competitive, molecular adsorption of hydrogen is assumed (as for the Ni/Al_2O_3 catalyst). Model 5 presented a slightly higher Rc value and consequently slightly smaller $(SSR)_{min}$ value than model 7. The latter model, however, exhibits a lower correlation between b_{H_2} and k_3 and between b_{H_2} and b_N than model 5 (see correlation matrices). Nevertheless, model 5 exhibits a smaller correlation coefficient between k_3 and b_N, showing the difficulty in discriminating the best between these two models. Both models present a slightly negative confidence interval for b_{H_2} (b_H) estimate. However, model 7 produced a clear narrower confidence interval for this estimate than model 5 and therefore, it can be concluded that, in a mathematical sense, it fitted better the experimental data than model 5. The hydrogen adsorption constant was found to be lower than the adsorption constant for naphthalene, as expected. A comparison between the values predicted by the L–H model 7 and the experimental data is illustrated in Fig. 5. Fig. 6 shows the parity plot illustrating the goodness of the fit and the 95% confidence interval for a normal distribution of the data (S_{td} = 5.0% for all regressed experimental data).

In summary, the surface reaction with the first addition of hydrogen (step III) was found to control the naphthalene HYD over the Ru/Al_2O_3 catalyst at 373.15 K. The hydrogen adsorbed molecularly on the surface, although the atomic adsorption of hydrogen cannot be completely ruled out as it also gave a good fit of the experimental data. Moreover, hydrogen adsorbed on different catalytic sites than naphthalene and therefore it did not compete with naphthalene for them.

3.4. Comparative analysis

The regression results, for the three catalysts studied, are summarized in Table 7. Comparing the estimated parameters from the L–H model for the Ru and Ni/Al_2O_3 catalysts, it can be observed that the adsorption constant for hydrogen and naphthalene were higher in the case of the Ru/Al_2O_3 catalyst. The adsorption constant for hydrogen was found to be around three times higher over the Ru/Al_2O_3 catalyst, whereas the naphthalene adsorption constant was roughly of the same order of magnitude. These results indicate that these reactants adsorbed stronger on the surface of this catalyst than on the surface of the Ni/Al_2O_3 catalyst. This was expected, as the orders of the reaction relative to these two reactants, reported by Monteiro-Gezork et al. [13], were lower in the case of the Ru/Al_2O_3 catalyst, indicating a higher surface coverage by them on this catalyst. The reaction rate constant was found to be around six times higher over the Ru/Al_2O_3 catalyst. All these results reinforce the results from Monteiro-Gezork et al. [13], i.e., that the Ru catalyst was a much more active catalyst towards naphthalene HYD than the Ni/Al_2O_3 catalyst.

Comparing both Ni and Ru catalysts with the $NiMo/Al_2O_3$ catalyst, both naphthalene and hydrogen adsorption constants were found to be lower in the latter catalyst than in the former two catalysts, being the difference more striking in the case of the hydrogen constant. The adsorption constant for hydrogen, over the $NiMo/Al_2O_3$ catalyst at 573.15 K, was found to be nearly 4 orders of magnitude lower than the adsorption constant over the Ru/Al_2O_3 catalyst. Therefore, the surface coverage by these reactants was higher over the Ni and Ru catalysts than over the $NiMo/Al_2O_3$ catalyst.

In summary, the adsorption strength of hydrogen and naphthalene increased as the catalyst activity towards naphthalene HYD increased, i.e., $Ru_{373.15\ K} > Ni_{373.15\ K} > NiMo_{523.15\ K} > NiMo_{573.15\ K}$. It has to be noted that the adsorption constants over the $NiMo/Al_2O_3$ were estimated at a much higher temperature than the Ni and Ru/Al_2O_3 catalysts and that a higher value would be expected at a lower temperature. However,

the reaction rate over the $NiMo/Al_2O_3$ catalyst at 523.15 K was already quite low and it was not possible to perform the reaction at such low temperature. For the three catalysts, the adsorption constant of naphthalene was found to be clearly higher than that of hydrogen, indicating that naphthalene molecules adsorbed more strongly on the surface of the catalyst than the hydrogen atoms or molecules, as expected.

4. Conclusions

Mechanistic L–H models, for the HYD of naphthalene, were derived and were tested by regressing the experimental data that translated the effect of both naphthalene and hydrogen concentration on the initial rate. The results showed that the reaction was controlled by the surface reaction and that the first surface addition of hydrogen (step III) was the limiting step. Hydrogen and naphthalene adsorbed on the same type of catalytic sites of the presulphided $NiMo/Al_2O_3$ catalyst, whereas the adsorption of these two reactants was found to take place on different sites of the Ni and Ru/Al_2O_3 catalysts. When the best mechanistic models were compared, the best fit, in a strictly mathematical sense, was obtained by assuming a molecular adsorption of hydrogen on the surface of the presulphided NiMo and prereduced Ni and Ru/Al_2O_3 catalysts. However, from a chemical point of view, the atomic adsorption could not be completely ruled out. This L–H model gave a good fit with physically meaningful parameters. The adsorption constant values indicate that naphthalene formed stronger bonds with the catalysts surface than the hydrogen. In addition, hydrogen and naphthalene were found to adsorb more strongly on the surface of the Ru/Al_2O_3 catalyst than on the surface of the Ni or the $NiMo/Al_2O_3$ catalysts. All these results emphasized the fact that the prereduced Ru catalyst was a much more active catalyst towards naphthalene HYD than the prereduced Ni/Al_2O_3 or the presulphided $NiMo/Al_2O_3$ catalyst.

Acknowledgements

The authors wish to acknowledge the financial support from Fundação para a Ciência e Tecnologia, Portugal, British Petroleum (BP), UK, and Universidad Autónoma del Estado de México.

Appendix A

Table A.1.

Table A.1
Langmuir–Hinshelwood-type rate equations derived from different controlling steps and tested for fitting the naphthalene hydrogenation initial reaction rate data

Surface reaction controls

Competitive, dissociative adsorption of hydrogen

Step III is rate determining

General expression:

$$r_3 = \frac{k'_3 C_N C_{H_2}}{(1+b_H^{1/4} C_{H_2}^{1/2} + b_N C_N + b_T C_T + K'_4 (C_T/C_{H_2})^3}$$

$$k'_3 = k_3 b_N b_H^{1/2}$$

$$K'_4 = \frac{b_T}{K_4 b_H^{1/2}}$$

Initial condition ($C_T \approx 0$):

$$r_3 = \frac{k'_3 C_N C_{H_2}}{(1+b_H^{1/4} C_{H_2}^{1/2} + b_N C_N)^3}$$

Model 1

Step IV is rate determining

$$r_4 = \frac{k'_4 C_N C_{H_2}^2}{(1+b_H^{1/4} C_{H_2}^{1/2} + b_N C_N + b_T C_T + K'_3 C_N C_{H_2})^3}$$

$$k'_4 = k_4 b_H^{1/2} K'_3 = k_4 b_H b_N K_3$$

$$K'_3 = K_3 b_N b_H^{1/2}$$

$$r_4 = \frac{k'_4 C_N C_{H_2}^2}{(1+b_H^{1/4} C_{H_2}^{1/2} + b_N C_N + K'_3 C_N C_{H_2})^3}$$

Model 2

Competitive, molecular adsorption of hydrogen

Step III is rate determining

General expression:

$$r_3 = \frac{k'_3 C_N C_{H_2}}{(1+b_{H_2}^{1/2} C_{H_2} + b_N C_N + b_T C_T + K'_4 (C_T/C_{H_2}))^2}$$

$$k'_3 = k_3 b_N b_{H_2}^{1/2}$$

$$K'_4 = \frac{b_T}{K_4 b_{H_2}^{1/2}}$$

Initial condition ($C_T \approx 0$):

$$r_3 = \frac{k'_3 C_N C_{H_2}}{(1+b_{H_2}^{1/2} C_{H_2} + b_N C_N)^2}$$

Model 3

Step IV is rate determining

$$r_4 = \frac{k'_4 C_N C_{H_2}^2}{(1+b_{H_2}^{1/2} C_{H_2} + b_N C_N + b_T C_T + K'_3 C_N C_{H_2})^2}$$

$$k'_4 = k_4 b_{H_2}^{1/2} K'_3 = k_4 b_{H_2} b_N K_3$$

$$K'_3 = K_3 b_N b_{H_2}^{1/2}$$

$$r_4 = \frac{k'_4 C_N C_{H_2}^2}{(1+b_{H_2}^{1/2} C_{H_2} + b_N C_N + K'_3 C_N C_{H_2})^2}$$

Model 4

Non-competitive, dissociative adsorption of hydrogen

Table A.1 (*Continued*)

Step III is rate determining

General expression:

$$r_3 = \frac{k'_3 C_N C_{H_2}}{(1+b_H^{1/4} C_{H_2}^{1/2})^2 (1+b_N C_N + b_T C_T + K'_4 (C_T/C_{H_2}))}$$

Initial condition ($C_T \approx 0$):

$$r_3 = \frac{k'_3 C_N C_{H_2}}{(1+b_H^{1/4} C_{H_2}^{1/2})^2 (1+b_N C_N)}$$

$$k'_3 = k_3 b_N b_H^{1/2}$$

Model 5

$$K'_4 = \frac{b_T}{K_4 b_H^{1/2}}$$

Step IV is rate determining

$$r_4 = \frac{k'_4 C_N C_{H_2}^2}{(1+b_H^{1/4} C_{H_2}^{1/2})^2 (1+b_N C_N + b_T C_T + K'_3 C_N C_{H_2})}$$

$$r_4 = \frac{k'_4 C_N C_{H_2}^2}{(1+b_H^{1/4} C_{H_2}^{1/2})^2 (1+b_N C_N + K'_3 C_N C_{H_2})}$$

$$k'_4 = k_4 b_H^{1/2} K'_3 = k_4 b_H b_N K_3$$

Model 6

$$K'_3 = K_3 b_N b_H^{1/2}$$

Non-competitive, molecular adsorption of hydrogen

Step III is rate determining

General expression:

$$r_3 = \frac{k'_3 C_N C_{H_2}}{(1+b_{H_2}^{1/2} C_{H_2})(1+b_N C_N + b_T C_T + K'_4 (C_T/C_{H_2}))}$$

Initial condition ($C_T \approx 0$):

$$r_3 = \frac{k'_3 C_N C_{H_2}}{(1+b_{H_2}^{1/2} C_{H_2})(1+b_N C_N)}$$

$$k'_3 = k_3 b_N b_{H_2}^{1/2}$$

Model 7

$$K'_4 = \frac{b_T}{K_4 b_{H_2}^{1/2}}$$

Step IV is rate determining

$$r_4 = \frac{k'_4 C_N C_{H_2}^2}{(1+b_{H_2}^{1/2} C_{H_2})(1+b_N C_N + b_T C_T + K'_3 C_N C_{H_2})}$$

$$r_4 = \frac{k'_4 C_N C_{H_2}^2}{(1+b_{H_2}^{1/2} C_{H_2})(1+b_N C_N + K'_3 C_N C_{H_2})}$$

$$k'_4 = k_4 b_{H_2}^{1/2} K'_3 = k_4 b_{H_2} b_N K_3$$

Model 8

$$K'_3 = K_3 b_N b_{H_2}^{1/2}$$

Adsorption of hydrogen controls

Competitive, dissociative adsorption of hydrogen

General expression:

$$r_2 = \frac{k_2 C_{H_2}^2}{(1+b_N C_N + b_T C_T + K'_3 C_N^{1/2} C_T^{1/2} + K'_4 (C_T/C_N)^{1/4})^4}$$

Initial condition ($C_T \approx 0$):

$$r_2 = \frac{k_2 C_{H_2}^2}{(1+b_N C_N)^4}$$

$$K'_3 = K_3 b_N \left(\frac{b_T}{K_4 K_3 b_N}\right)^{1/2}$$

Model 9

$$K'_4 = \left(\frac{b_T}{K_4 K_3 b_N}\right)^{1/4}$$

Competitive, molecular adsorption of hydrogen

General expression:

$$r_2 = \frac{k_2 C_{H_2}^2}{(1+b_N C_N + b_T C_T + K'_3 C_N^{1/2} C_T^{1/2} + K'_4 (C_T/C_N)^{1/2})^2}$$

Initial condition ($C_T \approx 0$):

$$r_2 = \frac{k_2 C_{H_2}^2}{(1+b_N C_N)^2}$$

$$K'_3 = K_3 b_N \left(\frac{b_T}{K_4 K_3 b_N}\right)^{1/2}$$

Model 10

$$K'_4 = \left(\frac{b_T}{K_4 K_3 b_N}\right)^{1/2}$$

Non-competitive, molecular adsorption of hydrogen

General expression:

$$r_2 = \frac{k_2 C_{H_2}^2}{(1+K'_4 (C_T/C_N)^{1/2})^2}$$

Initial condition ($C_T \approx 0$):

$$r_2 = k_2 C_{H_2}^2$$

$$K'_4 = \left(\frac{b_T}{K_4 K_3 b_N}\right)^{1/2}$$

Model 11

Non-competitive, dissociative adsorption of hydrogen

General Expression:

$$r_2 = \frac{k_2 C_{H_2}^2}{(1+K'_4 (C_T/C_N)^{1/4})^4}$$

Initial condition ($C_T \approx 0$)

$$r_2 = k_2 C_{H_2}^2$$

Table A.1 (*Continued*)

$K'_4 = \left(\frac{b_T}{K_4 K_3 b_N}\right)^{1/4}$	Model 11
Adsorption of naphthalene controls Competitive, dissociative adsorption of hydrogen	
General expression:	Initial condition ($C_T \approx 0$)
$r_1 = \frac{k_1 C_N}{(1+b_H^{1/4} C_{H_2}^{1/2} + K'_3(C_T/C_{H_2}^2) + b_T C_T + K'_4(C_T/C_{H_2}))}$	$r_1 = \frac{k_1 C_N}{1+b_H^{1/4} C_{H_2}^{1/2}}$
$K'_4 = \frac{b_T}{K_4 b_H^{1/2}}$	Model 12
$K'_3 = \frac{b_T}{K_4 K_3 b_H^{1/2}}$	
Competitive, molecular adsorption of hydrogen	
General expression:	Initial condition ($C_T \approx 0$)
$r_1 = \frac{k_1 C_N}{(1+b_{H_2}^{1/2} C_{H_2} + K'_3(C_T/C_{H_2}^2) + b_T C_T + K'_4(C_T/C_{H_2}))}$	$r_1 = \frac{k_1 C_N}{(1+b_{H_2}^{1/2} C_{H_2})}$
$K'_4 = \frac{b_T}{K_4 b_{H_2}^{1/2}}$	Model 13
$K'_3 = \frac{b_T}{K_4 K_3 b_{H_2}}$	
Non-competitive, molecular adsorption of hydrogen	
General expression:	Initial condition ($C_T \approx 0$):
$r_1 = \frac{k_1 C_N}{(1+K'_3(C_T/C_{H_2}^2) + K'_4(C_T/C_{H_2}) + b_T C_T)}$	$r_1 = k_1 C_N$
$K'_4 = \frac{b_T}{K_4 b_{H_2}^{1/2}}$	Model 14
$K'_3 = \frac{b_T}{K_4 K_3 b_{H_2}}$	
Non-competitive, dissociative adsorption of hydrogen	
General expression:	Initial condition ($C_T \approx 0$)
$r_1 = \frac{k_1 C_N}{(1+K'_3(C_T/C_{H_2}^2) + K'_4(C_T/C_{H_2}) + b_T C_T)}$	$r_1 = k_1 C_N$
$K'_4 = \frac{b_T}{K_4 b_H^{1/2}}$	Model 14
$K'_3 = \frac{b_T}{K_4 K_3 b_H}$	

References

[1] G.C. Schuit, B.C. Gates, AIChE J. 19 (1973) 417.
[2] M.L. Vrinat, Appl. Catal. 6 (1983) 137.
[3] E. Furimsky, Appl. Catal. A: Gen. 171 (1998) 177.
[4] T. Kabe, A. Ishihara, W. Qian, Hydrodesulfurization and Hydenitrogenation Chemistry and Engineering, Kodansha and Wiley-VCH, Tokyo, 1999
[5] R. Shafi, G.J. Hutchings, Catal. Today 59 (2000) 423.
[6] A. Avidan, B. Klein, R. Ragsdale, Hydrocarbon Process. 80 (2001) 47.
[7] K.G. Knudsen, D.D. Whitehurst, P. Zeuthen, A Detailed Understanding of the Inhibition Effect of Organic Nitrogen Compounds for Ultra Deep HDS and the Consequences for Choice of Catalyst, in: AIChE 2000 Spring National Meeting, Atlanta, 2000.
[8] M.F. Wilson, I.P. Fisher, J.F. Kriz, Ind. Eng. Chem. Prod. Res. Dev. 25 (1986) 505.
[9] M.F. Wilson, J.F. Kriz, Fuel 63 (1984) 190.
[10] Y. Kidoguchi, C. Yang, R. Kato, K. Miwa, J. Soc. Automative Eng. Jpn. 21 (2000) 469.
[11] B.H. Cooper, B.B.L. Donnis, Appl. Catal. A: Gen. 137 (1996) 203.
[12] A.C.A. Monteiro-Gezork, A. Effendi, J.M. Winterbottom, Catal. Today 128 (2007) 63.
[13] A.C.A. Monteiro, Hydrotreating: HDA Studies on NiMo- Ni- and Ru/Al_2O_3 Catalysts for the HYD of Naphthalene, PhD Thesis, The University of Birmingham, UK, 2005.
[14] P.R. Weisz, C.D. Prater, Adv. Catal. 6 (1954) 143.
[15] S. Smeds, D. Murzin, T. Salmi, Appl. Catal. A: Gen. 125 (1995) 271.
[16] S. Toppinen, T.-K. Rantakylä, T. Salmi, J. Aittamaa, Ind. Eng. Chem. Res. 35 (1996) 1824.
[17] P.A. Rautanen, J.R. Aittamaa, A.O.I. Krause, Ind. Eng. Chem. Res. 39 (2000) 4032.
[18] C. Mirodatos, J.A. Dalmon, G.A. Martin, J. Catal. 105 (1987) 405.
[19] D.W. Marquardt, SIAM J. Appl. Mathem. 11 (1963) 431.
[20] J.R. Kittrell, Adv. Chem. Eng. 8 (1970) 97.
[21] G.F. Froment, K.B. Bischoff, Chemical Reactor Analysis and Design, John Wiley & Sons, Singapore, 1990.
[22] H.S. Fogler, Elements of Chemical Reaction Engineering, Prentice-Hall International, London, 1999.
[23] G.E.P. Box, W.J. Hill, Technometrics 9 (1967) 57.
[24] G. Box, L.R. Connor, W.R. Cousins, O.L. Davies, F.R. Himsworth, G.P. Sillito, Design and Analysis of Industrial Experiments, Imperial Chemical Industries Limited., London, 1956.
[25] M.S. Lylykangas, P.A. Rautanen, A.O.I. Krause, Ind. Eng. Chem. Res. 41 (2002) 5632.
[26] P.A. Rautanen, M.S. Lylykangas, J.R. Aittamaa, A.O.I. Krause, Ind. Eng. Chem. Res. 41 (2002) 5966.
[27] P.A. Rautanen, J.R. Aittamaa, A.O.I. Krause, Chem. Eng. Sci. 56 (2001) 1247.
[28] L.P. Lindfords, T. Salmi, Ind. Eng. Chem. Res. 32 (1993) 34.